



The effect of variable liposome brightness on quantifying lipid–protein interactions using fluorescence correlation spectroscopy

Ana M. Melo ^a, Manuel Prieto ^a, Ana Coutinho ^{a,b,*}

^a Centro de Química-Física Molecular and Institute of Nanoscience and Nanotechnology, Instituto Superior Técnico, U.T.L, Complexo I, Av. Rovisco Pais, 1049-001 Lisboa, Portugal

^b Dep. Química e Bioquímica, FCUL, Campo Grande, 1749-016 Lisboa, Portugal

ARTICLE INFO

Article history:

Received 15 February 2011

Received in revised form 1 June 2011

Accepted 1 June 2011

Available online 12 June 2011

Keywords:

Membrane partition

Molecular brightness

Poisson distribution

Lysozyme

Anionic phospholipid vesicles

Electrostatic interaction

ABSTRACT

Fluorescence correlation spectroscopy (FCS) has been increasingly used to study the binding of fluorescently-labeled peptides and proteins to phospholipid vesicles. In this work, we present a new method to analyze partition data obtained by this technique based on the assumption that the number of fluorescently-labeled protein molecules bound per liposome follows a Poisson distribution. To not overestimate the recovered partition coefficients, we first show that the variation in liposome brightness caused by this statistical distribution must be considered explicitly in data analysis when the parameter used to establish the partition curves is the fractional instead of the absolute amplitudes associated with the slowest diffusing particles in the system (lipid vesicles), a choice frequently made in FCS partition studies. We further extend the theoretical model describing the membrane partition of a fluorescently-labeled protein by considering the presence of a trace amount of free fluorescent dye (non-binding component) in the system. We show that this situation can account for an apparent maximal binding level lower than 100% in the experimental partitioning curves obtained for Alexa 488 fluorescently-labeled lysozyme and liposomes prepared with variable anionic phospholipid content. The extreme sensitivity of the FCS technique allowed uncoupling lysozyme partition from the protein-induced liposome aggregation, confirming that lysozyme binding to negatively charged liposomes is dominantly driven by electrostatic interactions.

© 2011 Elsevier B.V. All rights reserved.

1. Introduction

Lipid–protein interactions are required to maintain cell functions and viability and are involved in a wide range of cellular processes, such as cell signaling events [1,2]. The reversible recruitment of cytosolic proteins to the membranes through the establishment of electrostatic interactions with acidic phospholipids, and particularly with specific phosphoinositides, is a common mechanism to these processes [3,4]. On the other hand, several *in vitro* studies have shown that the surface of negatively-charged lipid membranes can induce the pathological self-assembly of numerous amyloidogenic and non-amyloidogenic peptides and proteins, resulting in amyloid fiber formation [5–8]. The potentially high concentration of peptides/proteins (surface crowding) reached at the membrane-surface

due to electrostatically-driven peptide/protein membrane interactions, combined with the low dimensionality of the interface, are expected to enhance the contact probability between partially unfolded peptides/proteins, which may lead to faster clustering, and amyloid-like fiber formation [5,6]. Quantitative evaluation of peptide/protein binding to liposomes through the determination of their partition coefficients should therefore be the first key step in the elucidation of the role of lipid membranes in their fibrillation mechanism. In fact, these equilibrium constants allow the calculation of protein interfacial coverage of the lipid vesicles, often the critical parameter controlling the peptide/protein membrane binding mode (peripheral *versus* partial insertion) [9] and its conformational/oligomerization state [8].

Among the wide variety of spectroscopic techniques that have been employed in the determination of peptide/protein partition coefficients [10], fluorescence correlation spectroscopy (FCS) has recently emerged as an important alternative [11,12]. FCS is a technique with single molecule sensitivity that analyzes fluctuations in fluorescence over time within a small observation volume. These fluctuations arise from a change in the average number of independently moving fluorescent particles in the confocal observation volume and from transitions to a dark state [13,14]. Autocorrelation (AC) analysis of FCS fluctuation data can be used to measure concentrations, translational diffusion properties, chemical reactions and binding processes undergone by the individual fluorescent molecules present in the sample [15,16].

Abbreviations: AC, autocorrelation; Alexa 488, Alexa Fluor 488 (carboxylic acid, succinimidyl ester, mixed isomers, dilithium salt); Alexa488-lysozyme, lysozyme conjugated with the fluorescent dye Alexa Fluor 488; BODIPY-PC, 2-(4,4-difluoro-5methyl-4-bora-3a,4a-diaza-s-indacene-3-dodecanoyl)-1-hexadecanoyl-*sn*-glycero-3-phosphocholine; BSA, bovine serum albumin; FCS, fluorescence correlation spectroscopy; LUV, large unilamellar vesicles; POPC, 1-palmitoyl-2-oleoyl-*sn*-glycero-3-phosphocholine; POPS, 1-palmitoyl-2-oleoyl-*sn*-glycero-3-phosphoserine

* Corresponding author at: Centro de Química-Física Molecular and Institute of Nanoscience and Nanotechnology, Instituto Superior Técnico, U.T.L, Complexo I, Av. Rovisco Pais, 1049-001 Lisboa, Portugal. Tel.: +351 21 8419248; fax: +351 21 8464455.

E-mail address: ana.coutinho@ist.utl.pt (A. Coutinho).

In this work, we describe the application of FCS to membrane partition studies by investigating the interaction between lysozyme labeled with Alexa Fluor 488 (Alexa488-lysozyme) and liposomes prepared with variable anionic phospholipid content as a model system. Lysozyme is a stable, highly basic small globular protein with a well-known 3D structure [17]. In addition to its known catalytic action, the lipid-binding properties of lysozyme have also been recently implicated in its bactericidal role [18]. Furthermore, phosphatidylserine-containing membranes have also been proposed to be able to induce the formation of “amyloid-like” fibrils by different non-amyloidogenic proteins, including lysozyme among others [19–21].

In this study, we highlight some potential pitfalls in data analysis that can lead to an overestimation of protein's partition coefficients measured using single color FCS. The observable species that are distinguishable in a FCS partition study, characterized by very different diffusion coefficients, are only two: the free fluorescently-labeled protein and the lipid vesicles with one or more bound conjugated proteins. In a multicomponent system the measured AC function is a weighted sum of the AC functions of each component, with amplitudes proportional to the square of the molecular brightness of the diffusing particles detected [22]. Taking this consideration into account, we will show first the need to consider explicitly the statistical (Poissonian) distribution of conjugated proteins bound per liposome when the experimental AC curves are analyzed using a fitting function with fractional instead of absolute amplitudes, an aspect that is largely overlooked in the literature. Secondly, we will illustrate how the presence of a trace amount of free fluorescent dye in the system (non-binding component) can produce an apparent maximum binding level lower than 100% in the experimental partitioning curves and, consequently, affect the recovered protein partition coefficients. The extreme sensitivity of the FCS technique allowed lysozyme partition measurements to be uncoupled from the potential interfering lysozyme-induced liposome aggregation, confirming that lysozyme binding to negatively charged liposomes is dominantly driven by electrostatic interactions.

2. Materials and methods

2.1. Materials

1-Palmitoyl-2-oleoyl-*sn*-glycero-3-phosphocholine (POPC) and 1-palmitoyl-2-oleoyl-*sn*-glycero-3-phosphoserine (POPS) were obtained from Avanti Polar Lipids (Alabaster, AL). Lysozyme (EC 3.2.1.17) from chicken egg white was purchased from Fluka Biochemika (Buchs, Switzerland). Alexa Fluor 488 SE (carboxylic acid, succinimidyl ester, mixed isomers, dilithium salt) (Alexa 488), 2-(4,4-difluoro-5-methyl-4-bora-3a,4a-diaza-s-indacene-3-dodecanoyl)-1-hexadecanoyl-*sn*-glycero-3-phosphocholine (BODIPY-PC) and rhodamine 110 were obtained from Molecular Probes, Invitrogen (Eugene, OR). Distilled water (>18 M Ω /cm) was produced using a Millipore (Billerica, MA) system and used throughout the work.

2.2. Fluorescent labeling of lysozyme

Lysozyme was covalently labeled with Alexa 488 succinimidyl ester dye on the amine groups as described (using a 2-fold molar excess of the dye relatively to lysozyme at pH 8.3) [23]. Alexa488-lysozyme was separated from unreacted free probe by gel filtration through a Sephadex G-25 gel filtration column (30.5 \times 1.6 cm) equilibrated in 20 mM HEPES-KOH, 0.1 mM EDTA, pH 7.4 buffer. A dye-to-protein molar ratio, *D/P*, of 0.67 was estimated spectrophotometrically using the extinction coefficient of the dye provided by the supplier [24] and that of lysozyme in the UV [25]. Other labeling conditions were also explored in this work, namely using an equimolar dye-to-protein ratio in the reaction mixture, or lowering its pH to 7.5. In these cases, the final *D/P* obtained was 0.21 and 0.50, respectively.

2.3. Liposome preparation

Large unilamellar vesicles (LUV, ~100 nm diameter) containing POPC mixtures with 10, 20, 30 or 50 mol% POPS were prepared by the standard extrusion technique [26] using 20 mM HEPES-KOH, 0.1 mM EDTA, pH 7.4 buffer as described elsewhere [23]. Lipid vesicles were usually used within 2 days of preparation but they were found to be structurally stable for at least 5 days when stored at 4 °C. Fluorescent lipid vesicles were prepared by the addition of a small amount of BODIPY-PC to the phospholipid mixture (1:10 000 labeled-phospholipid/total lipid molar ratio).

2.4. Alexa 488 (free dye) binding assays to lysozyme

Alexa 488 (free dye) titration was performed by adding increasing concentrations of lysozyme to a fixed amount of free dye (0.1 μ M) after its reaction with hydroxylamine. After an incubation period of 30 min, the steady-state fluorescence intensity and anisotropy of the samples were measured on a SLM-AMINCO 8100 spectrofluorometer (Rochester, NY) using quartz cuvettes of 5 \times 5 mm path length. The steady-state anisotropy, $\langle r \rangle$, defined by:

$$\langle r \rangle = \frac{I_{VV} - GI_{VH}}{I_{VV} + 2GI_{VH}} \quad (1)$$

was obtained by measuring the vertically (parallel) and horizontally (perpendicular) polarized components of the fluorescence emission with the excitation polarized vertically. The *G* factor ($G = I_{HV}/I_{HH}$) corrects for bias in the transmissivity between vertically and horizontally polarized components of the emission introduced by the detection system. Samples were excited at 480 nm, and the polarized emission was detected at 512 nm, both with a bandwidth of 8 nm. Background intensities were always taken into account and subtracted from the measured sample intensities.

Assuming a 1:1 stoichiometry, and that the protein is present in large excess over the ligand, Eq. (2) was fitted to the experimental data of fluorescence intensity, *I*, versus total protein concentration, $[P]_t$, by non-linear least squares regression to determine the protein–ligand dissociation constant, K_d :

$$I = I_f - \frac{\Delta I_{\max} \cdot [P]_t}{K_d + [P]_t} \quad (2)$$

where I_f and I_b are the fluorescence intensities of the free and bound ligand, respectively, and $\Delta I_{\max} = I_f - I_b$. The fluorescence anisotropy binding curve of Alexa 488 to lysozyme was also used to determine K_d by fitting Eq. (3) to the experimental data of $\langle r \rangle$ versus $[P]_t$:

$$\langle r \rangle = \frac{F \cdot \langle r \rangle_f \cdot (K_d + [P]_t) + (\langle r \rangle_b - F \cdot \langle r \rangle_f) \cdot [P]_t}{F \cdot (K_d + [P]_t) + (1 - F) \cdot [P]_t} \quad (3)$$

where $\langle r \rangle_f$ and $\langle r \rangle_b$ are the steady-state fluorescence anisotropies of the free ligand and ligand–protein complex, respectively, and *F* is the fluorescence quenching factor of the Alexa 488 dye after its non-covalent binding to lysozyme ($F = I_f/I_b$).

2.5. Fluorescence correlation spectroscopy

2.5.1. FCS instrumentation

FCS measurements were carried out on a FCS setup based on a dual channel ISS Alba fluorescence correlation detector with avalanche photodiodes connected to a Leica SP5 TCS confocal inverted microscope (Leica Microsystems, Wetzlar, Germany). The 488-nm line provided by an Argon laser was focused into the sample by an apochromatic water immersion objective (63 \times , NA 1.2; Zeiss, Jena, Germany). The emission was detected confocally after passing through a 500–550 band-pass filter. A 111.44 μ m diameter pinhole in the image

plane blocked out-of-focus signals. Partition studies were made using a constant concentration of Alexa488-conjugated lysozyme and by varying the total lipid concentration in solution. Each measurement consisted of 10 AC curves of 20 s each, acquired with a sampling frequency of 200 or 500 kHz. FCS measurements were carried out using 8-well chamber slides (Ibidi, Martinsried, Germany). To prevent nonspecific adsorption of Alexa488-lysozyme, the chamber wells were precoated with a 10% bovine serum albumin (BSA) solution and the samples were loaded after extensive rinsing with buffer. The fluorescence was recorded from the confocal volume located ~200 μm above the top surface of the cover slide. The focus volume (0.21 fl) was determined by calibration with 5 and 10 nM rhodamine 110 in buffer solution measured under the same illumination conditions as the samples and considering $D_{\text{Rhodamine 110}} = 440 \mu\text{m}^2 \text{s}^{-1}$ [27].

2.5.2. Analysis of the experimental AC curves

Data analysis of the experimental AC curves was performed using the ISS Vista software. This program uses a Marquardt–Levenberg nonlinear least-squares fitting routine and the goodness of the fittings can be judged by the recovered χ^2 and random distribution of the weighted residuals.

The AC function for single fluorescent particles is given by [14]:

$$G(\tau) = G_T(\tau) \cdot G_D(\tau) \quad (4)$$

with

$$G_D(\tau) = \frac{1}{N} \cdot \left(1 + \frac{\tau}{\tau_D}\right)^{-1} \cdot \left(1 + \frac{\tau}{S^2 \tau_D}\right)^{-1/2} \quad (5.A)$$

and

$$G_T(\tau) = 1 + \frac{T}{1-T} \cdot \exp\left(-\frac{\tau}{\tau_T}\right). \quad (5.B)$$

$G_D(\tau)$ and $G_T(\tau)$ are the parts of the correlation function for translational diffusion and triplet-state formation, respectively. N is the average number of fluorescent molecules in the laser focus volume, T and τ_T are the fraction of fluorophores in the triplet state and their triplet lifetime, respectively, and τ_D is the translational diffusion time of the particles. This correlation time is the characteristic average diffusional transit time during which a molecule resides in the observation volume with the axial (ω_z) to lateral (ω_{xy}) dimension ratio $S (= \omega_z / \omega_{xy})$ and equals $\tau_D = \omega_{xy}^2 / 4D$, where D is the diffusion coefficient. For one-component samples (model M1), Eq. (4) was globally fitted to the experimental data by linking the triplet and diffusing times (τ_T and τ_D , respectively) across all the AC curves obtained for each sample. In the analysis, a three-dimensional Gaussian model was selected for describing the laser point spread function and the structural parameter S obtained in the calibration procedure using 5 and 10 nM rhodamine 110 in buffer solution ($S = 5.9 \pm 0.5$) was subsequently fixed for the other samples measured in the same chamber slide.

In the partition studies, Eq. (6) was used to fit the experimental AC curves, either by considering a two-component (model M2: free Alexa488-conjugated lysozyme ($i = 1 = P$) and lipid vesicles with one or more bound fluorescently-labeled proteins ($i = 2 = ves$)) or a three-component system (model M3: free Alexa Fluor 488 dye present in solution ($i = 1 = Dye$), free Alexa488-conjugated lysozyme ($i = 2 = P$) and lipid vesicles with at least one fluorescently-labeled protein bound ($i = 3 = ves$)):

$$G(\tau) = \frac{1}{\langle N \rangle} \cdot \left(1 + \frac{T_1}{1-T_1} \cdot \exp\left(-\frac{\tau}{\tau_{T1}}\right)\right) \cdot \left(1 + \frac{T_2}{1-T_2} \cdot \exp\left(-\frac{\tau}{\tau_{T2}}\right)\right) \times \sum_{i=1}^3 f_i \left(1 + \frac{\tau}{\tau_{D_i}}\right)^{-1} \cdot \left(1 + \frac{\tau}{S^2 \tau_{D_i}}\right)^{-1/2}. \quad (6)$$

In this equation, T_i is the fraction of fluorescent component i in the triplet state, τ_{T_i} and τ_{D_i} are their triplet and diffusion lifetimes, respectively, and f_i is its fractional contribution to the AC function (with $f_2 = 1 - f_1$ and $f_3 = 1 - f_1 - f_2$ for the two- and three component models, respectively). To reduce the strong statistical correlations among the fit parameters, the FCS data was globally analyzed by linking the diffusing time associated with the slowest component (liposomes with bound fluorescently-labeled proteins) between all the AC curves obtained for each sample. Additional parameters, such as the triplet relaxation and diffusion times associated with the free dye and Alexa488-conjugated protein were fixed at their known values measured previously in calibration (one-component) measurements.

2.5.3. Determination of membrane partition coefficients from FCS binding data

To take into account the Poisson distribution of the fluorescently-labeled lysozyme among the lipid vesicles in the determination of the partition coefficients (see the Theory section), the experimental partition curves (fractional amplitudes as a function of the accessible lipid concentration) were fitted by a nonlinear least-squares procedure using the Solver Add-in of the Microsoft Excel spreadsheet program (Microsoft, Redmond, WA). The precision of the fitted parameters was estimated using the macros Solver Statistics. The calculations performed in the fitting procedure always considered a three-component system (model M3: free Alexa Fluor 488 dye, free Alexa488-labeled lysozyme and liposomes containing at least one fluorescently-labeled protein bound). Values for the partition coefficient and concentration of free dye present in each sample, K_p and $[Dye]$, respectively, were initially guessed and the average number of membrane-bound proteins per lipid vesicle, $\langle k \rangle$, was calculated for each lipid concentration using Eqs. (9) and (13). The average number of lipid molecules in a liposome, μ , was calculated to be 100,000 considering that each phospholipid head group occupies an average surface area of 0.63 nm^2 [28] and that the liposomes were prepared by extrusion using filters with 100 nm pores. The probabilities of finding a lipid vesicle with k proteins ($k = 1, 2, \dots$) were then computed using Eq. (10) and, finally, f_{ves}^{M3} was obtained using Eq. (20) by assuming that the ratio between the brightness of the free dye and the Alexa488-covalently labeled lysozyme, q , was 1.9. These calculated fractional amplitudes were then compared to the experimental values, and the sum of their weighted square deviations was minimized using Solver in an iterative procedure by changing the initially guessed K_p and $[Dye]$ values. The experimental fractional amplitudes used in the fitting procedure were either f_2 or f_3 , i.e., the fractional amplitudes associated with the slowest diffusion component (liposomes with fluorescently-labeled proteins bound) obtained from a two- or three-component analysis of the experimental AC curves using Eq. (6), respectively, as described in the previous section. The different partition curves obtained for the same protein batch using variable mol% of POPS in the preparation of the liposomes were globally analyzed by linking the value of $[Dye]$ between all the curves used in the fitting procedure.

3. Theory

The AC function for multiple independent fluorescent species is a linear combination of the autocorrelations curves for each species, weighted by the square of their respective molecular brightness's, B_i , [22]:

$$G_D(\tau) = \sum_{i=1}^n B_i^2 N_i^2 G_{D_i}(\tau) / \left[\sum_{i=1}^n B_i N_i \right]^2 \quad (7)$$

where N_i and $G_{D_i}(\tau)$ are the mean particle number and the translational diffusion part of the AC curve for the i th species (Eq. (4)),

respectively. The brightness of each species depends on its absorption cross-section, fluorescence quantum yield and detection efficiency in the confocal microscope. Considering q_i the ratio of the brightness of the i th component to that of a given component chosen as a reference and $G_{Di}(\tau) = 1/N_i \cdot g_i(\tau)$, we obtain:

$$G_D(\tau) = \frac{1}{N_{av}} \cdot \sum_{i=1}^n A_i \cdot g_i(\tau) \quad (8)$$

$$\text{with } N_{av} = \sum_{i=1}^n q_i N_i \text{ and } A_i = q_i^2 N_i / \left(\sum_{i=1}^n q_i N_i \right).$$

Usually, in a partition experiment, the only two observable species in a FCS measurement are the fast-diffusing free fluorescently-labeled protein (*index P*) and the much larger, slower moving lipid vesicles with one or more bound fluorescently-labeled proteins (*index ves*) (two-component model, M2). Assuming that (i) protein binding to the lipid vesicles is non-cooperative, the mole fraction of the fluorescently-conjugated protein bound through hydrophobic/electrostatic interactions to the liposomes, x_m , is given by:

$$x_m = \frac{K_p \cdot [L]_{ac}}{[W] + K_p \cdot [L]_{ac}} \quad (9)$$

where K_p is the mole fraction partitioning coefficient [29], $[L]_{ac}$ is the accessible lipid concentration (half of the total lipid concentration used in each sample) and $[W]$ is the water concentration. Furthermore, considering that (ii) the protein distributes randomly among the liposomes according to a Poisson distribution [30], the probability of finding a lipid vesicle with k bound proteins is given by:

$$P(k, \langle k \rangle) = \frac{\langle k \rangle^k e^{-\langle k \rangle}}{k!} \quad (10)$$

where $\langle k \rangle$ is the average number of membrane-bound proteins per lipid vesicle.

The probability of finding liposomes without a membrane-bound protein is then,

$$P(0, \langle k \rangle) = e^{-\langle k \rangle} \quad (11)$$

and the overall number of lipid vesicles with at least one protein bound, N_{ves}^p , is given by:

$$N_{ves}^p = N_{ves}^t (1 - P(0, \langle k \rangle)) \cong N_{ves}^t \sum_{k=1}^l \frac{\langle k \rangle^k e^{-\langle k \rangle}}{k!} \quad (12)$$

where N_{ves}^t and N_{ves}^0 are the total number of lipid vesicles present in solution and protein-free liposomes, respectively ($N_{ves}^t = N_{ves}^0 + N_{ves}^p$). The Poisson distribution was approximated by a finite sum with a cut-off l set to 20 to guarantee that under the experimental conditions used $\sum_{k=1}^l P(k, \langle k \rangle) \cong 1$. Further assuming that (iii) the liposome population is monodisperse and its morphology is not affected by its protein occupancy number, $\langle k \rangle$ can be calculated from:

$$\langle k \rangle = \frac{x_m [P]_t \mu}{[L]_t} \quad (13)$$

where $[P]_t$ and $[L]_t$ are the total protein and lipid concentrations present in each sample, respectively, and μ is the average number of lipid molecules in a liposome. Finally, (iv) if the protein exchange among the liposomes is very slow during their diffusion time through the confocal volume (frozen exchange regime [31]), then a two-species model can be applied to describe the experimental AC curves obtained in a partition experiment.

According to Eq. (8), and further assuming that (v) the brightness of the conjugated protein does not change upon its binding to the

liposomes, the absolute amplitudes of each diffusing particle are given by Eqs. (14.A) and (14.B), respectively:

$$A_p^{M2} = \frac{N_p^f}{N_p^f + \left(\sum_{k=1}^l k \cdot P(k, \langle k \rangle) \right) \cdot N_{ves}^t} \quad (14.A)$$

and

$$A_{ves}^{M2} = \frac{\left(\sum_{k=1}^l k^2 \cdot P(k, \langle k \rangle) \right) \cdot N_{ves}^t}{N_p^f + \left(\sum_{k=1}^l k \cdot P(k, \langle k \rangle) \right) \cdot N_{ves}^t} \quad (14.B)$$

where N_p^f is the mean number of conjugated proteins that remain free in solution. Eq. (14.A) shows that the amplitude of the AC function associated with the fast diffusing species equals the mole fraction of free protein, x_f , and therefore $x_m = 1 - A_p^{M2}$. However, using Eqs. (14.A) and (14.B), it can be deduced that:

$$A_{ves}^{M2} = B \cdot x_m \quad (15)$$

with $B = \frac{\sum_{k=1}^l k^2 \cdot P(k, \langle k \rangle)}{\sum_{k=1}^l k \cdot P(k, \langle k \rangle)}$. The presence of the k^2 factor in the numerator of this parameter makes A_{ves}^{M2} equivalent to x_m only if an infinite diluted regime is achieved experimentally, i.e. when each vesicle contains no more than a single bound protein, as already discussed by Rusu et al. [11] and Posokhov et al. [12]. This stems from the fact that a lipid vesicle with two fluorescently-labeled proteins is exactly twice as bright as a liposome with a single protein, and it will contribute four times as much to the two-component AC function. In other words, as the total lipid concentration in solution is increased during a partition experiment, the B factor decreases, progressively approaching its limiting value of 1 at infinite dilution.

The fitting functions most commonly available in the software programs used in the analysis of the experimental AC curves make use of fractional, f_i , instead of absolute amplitudes, A_i , as weighting factors:

$$G_D(\tau) = \frac{1}{\langle N \rangle} \cdot \sum_{i=1}^n f_i \cdot g_i(\tau) \quad (16)$$

with $\sum_{i=1}^n f_i = 1$.

In a partition experiment:

$$\frac{1}{\langle N \rangle} = \frac{N_p^f + \sum_{k=1}^l k^2 \cdot P(k, \langle k \rangle)}{(N_p^t)^2} \quad (17)$$

where N_p^t is the total number of protein molecules present in solution.

According to Eqs. (14.A) and (14.B), the following expressions can be deduced for the fractional amplitudes associated with each species:

$$f_p^{M2} = \frac{N_p^f}{N_p^f + \left(\sum_{k=1}^l k^2 \cdot P(k, \langle k \rangle) \right) \cdot N_{ves}^t} \quad (18.A)$$

and

$$f_{ves}^{M2} = \frac{\left(\sum_{k=1}^l k^2 \cdot P(k, <k>) \right) \cdot N_{ves}^t}{N_p^f + \left(\sum_{k=1}^l k^2 \cdot P(k, <k>) \right) \cdot N_{ves}^t} \quad (18.B)$$

4. Results

4.1. Simulation of the outcome of a FCS partitioning experiment – two-component model

Before investigating Alexa488-conjugated lysozyme binding to liposomes prepared with a variable mole fraction of POPS, we tested the influence of the type of fitting function used in the analysis of the experimental AC curves on the recovered partition coefficients. Taking into account the set of assumptions described in the Theory section, and considering that the extruded lipid vesicles have on average 100,000 phospholipid molecules per liposome, we simulated the outcome of an FCS partition experiment for different input K_p values by calculating the variation of the absolute, A_i^{M2} , and fractional, f_i^{M2} , amplitudes (associated with the fast and slow diffusing species i) with the accessible lipid concentration present in each sample. The results obtained in these simulations for 10 nM of a fluorescently-labeled protein having a partition coefficient of 1×10^6 are exemplified in Fig. 1C. This figure shows that the values calculated for $1 - A_p^{M2}$ and f_{ves}^{M2} differ considerably when the lipid concentrations used in the simulated partition study are low ($[L]_{ac} \leq 0.5$ mM). For higher lipid

concentrations, these two parameters progressively converged, until their values became almost super-imposable for $[L]_{ac} \geq 1$ mM. In this situation, more than 95% of the fluorescently-labeled protein was bound to the liposomes and the “infinite dilution regime”, as described by Posokhov and co-workers [12], was attained. The excess of lipid in solution caused the average number of membrane-bound proteins per lipid vesicle, $\langle k \rangle$, to be much lower than 1 (Fig. 1A) and the B factor converged asymptotically to 1. On the contrary, when the total lipid concentration used in the simulated partition assays was less than 1 mM, the probability of finding multiple proteins simultaneously bound to a single liposome increased rapidly (Fig. 1B), although most of the protein present in each sample remained free in solution. These liposomes are brighter than the single-occupied ones and therefore strongly contribute to the experimentally measured AC curve (Eq. (18.B)), being responsible for the difference registered between $1 - A_p^{M2}$ and f_{ves}^{M2} at these low lipid concentrations. As expected, when the resulting partition curve of $1 - A_p^{M2}$ versus $[L]_{ac}$ was fitted to a mole fraction partitioning equilibrium described by Eq. (9), the correct input partition coefficient used in the simulation was recovered (Fig. 1C), confirming that $x_m = 1 - A_p^{M2}$. However, the partition curve obtained by representing f_{ves}^{M2} as a function of the accessible lipid concentration was no longer hyperbolic and a K_p value of 8.5×10^6 , almost one order of magnitude higher than the input value used in the simulation ($K_p^{input} = 1 \times 10^6$), was obtained from forcing the fitting of Eq. (9) to the simulated data (Fig. 1C and Table 1). These results clearly show that the common assumption, often considered in the analysis of FCS data obtained in a lipid–protein partition experiment, that the fractional amplitudes of the AC curves associated with the slow diffusing species (liposomes) are equivalent to the membrane-bound protein mole fraction is not valid, unless the

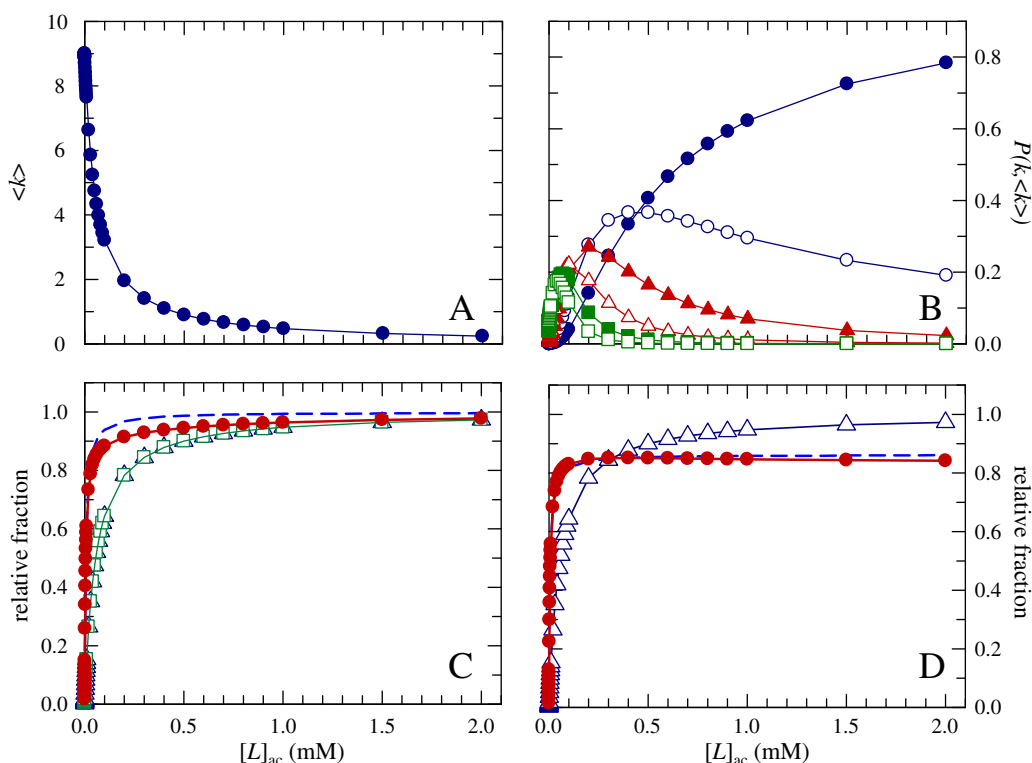


Fig. 1. Simulated protein partition curves as measured by FCS for (C) a two- and (D) a three-component system, respectively. Dependence of (A) the average number of membrane-bound proteins per lipid vesicle, $\langle k \rangle$ (●), (B) the Poisson probability of finding liposomes with k proteins, $P(k, \langle k \rangle)$ ($k=0$ (●); $k=1$ (○); $k=2$ (▲); $k=3$ (△); $k=4$ (■) and $k=5$ (□)) and (C and D) the mole fraction of membrane-bound protein, x_m (△), $1 - A_p^{M2}$ (□) and f_{ves}^{M2} (●) on the accessible lipid concentration in the sample. (C) The green line is the best fit of Eq. (9) to the data of $1 - A_p^{M2}$ versus $[L]_{ac}$ ($K_p^{fitted} = 1 \times 10^6$); (D) The solid blue line is just a guide to the eye. (C and D) The dashed blue lines are the best fits of Eqs. (9) and (21) to the data of (C) f_{ves}^{M2} and (D) f_{ves}^{M3} versus $[L]_{ac}$, respectively, yielding the results listed in Table 1. The red lines are the best fits to the simulated data of the mole fraction partitioning model explicitly considering (C) the Poisson distribution of 10 nM fluorescently-labeled protein among the liposomes ($\mu = 100,000$) and (D) the additional presence of 0.5 nM nonbinding species with $q = 2$. These fits yielded the same K_p as the input value used in the simulation ($K_p^{input} = 1 \times 10^6$) (see the text and Table 1 for more details).

Table 1

Analysis of the FCS protein partition curves obtained in the simulation of a two- and three-component system according to a simple mole-fraction partitioning equilibrium (see the text for more details).

K_p^{input}	Two-component system		Three-component system				
	$K_p^{\text{fitted a}}$	χ^2	$K_p^{\text{fitted b}}$	χ^2	$K_p^{\text{fitted c}}$	$x_{\text{m}}^{\text{max}}$	χ^2
5×10^4	6.4×10^4	4.4×10^{-5}	4.7×10^4	2.1×10^{-5}	7.5×10^4	0.78	1.2×10^{-6}
1×10^5	1.5×10^5	2.6×10^{-4}	1.0×10^5	9.8×10^{-4}	1.9×10^5	0.78	8.9×10^{-6}
5×10^5	2.1×10^6	1.2×10^{-3}	1.5×10^6	6.5×10^{-3}	2.8×10^6	0.83	9.8×10^{-7}
1×10^6	8.5×10^6	1.1×10^{-3}	6.4×10^6	6.9×10^{-3}	1.0×10^7	0.86	6.6×10^{-5}

^a Eq. (9) was used to fit the simulated data of $f_{\text{ves}}^{\text{M2}}$ versus $[L]_{\text{ac}}$.

^b Eq. (9) was used to fit the simulated data of $f_{\text{ves}}^{\text{M3}}$ versus $[L]_{\text{ac}}$.

^c Eq. (21) was used to fit the simulated data of $f_{\text{ves}}^{\text{M3}}$ versus $[L]_{\text{ac}}$.

FCS measurements are always carried out under the “infinite dilution regime”. In order to correctly use the experimental fractional amplitudes, f_2 , in the determination of K_p , the Poissonian distribution of the fluorescently-labeled protein among the lipid vesicles must be considered explicitly in the fitting procedure (see Section 2.5.3). This allows to account for the fact that when the data points are collected at low lipid concentrations the particles detected with the slow diffusing time have a variable brightness, depending on the number of proteins bound per vesicle, even when the protein binding to the liposomes does not change its fluorescence quantum yield, as it is shown in Fig. 1C. This effect is particularly important for peptides or proteins that establish strong electrostatic interactions with anionic lipid membranes, presenting high K_p values (Table 1).

4.2. Using FCS to monitor Alexa488-lysozyme binding to liposomes

Fig. 2A shows the normalized AC curves obtained for freely diffusing lysozyme conjugated with Alexa 488 ($D/P=0.67$) and for POPC:POPS 80:20 liposomes containing 0.01 mol% of BODIPY-PC. Eq. (4) (one-component model) was used to fit the AC curves measured with the fluorescently-labeled protein, and a diffusion time of $93 \pm 9 \mu\text{s}$ ($n=55$) was obtained. The experimental AC functions obtained for the POPC lipid vesicles prepared with 20 mol% of POPS showed that the extruded liposomes were monodisperse on FCS grounds presenting an average diffusion time of $\tau_{\text{ves}} = 1.5 \pm 0.1 \text{ ms}$ ($n=5$). Using the Stokes–Einstein relationship, an average hydrodynamic diameter of 81 nm can be calculated for these lipid vesicles. We measured small variations in τ_{ves} depending upon the composition of the vesicles but overall their hydrodynamic diameter was within the range expected for liposomes prepared by extrusion using 100 nm pores.

The curves in Fig. 2A clearly show that the AC curve of 10 nM Alexa488-labeled lysozyme decays on a longer time scale upon increasing the total lipid concentration in solution, causing an increase of the diffusion time as the conjugated protein molecules stay longer in the observation volume. A two-component model (model M2) was required to fit these AC curves (Fig. S1A published as Supporting Information). In the fitting procedure, the diffusion time of the first component, τ_1 , was fixed to the value previously determined for the free fluorescently conjugated protein, whereas the diffusion time of the second component, τ_2 , was linked across a data set. For the experiment presented in Fig. 2B, this diffusion time was found to be $\tau_2 = (1.4 \pm 0.1) \text{ ms}$ ($n=14$) and can thus be assigned to the slow diffusing liposomes with fluorescent protein molecules bound as expected. There was no systematic effect of the bound protein mass on the diffusion time of the liposomes, τ_2 , which indicates that the size of the lipid vesicles was not significantly affected as more fluorescently-labeled proteins were bound to the vesicles.

The binding of Alexa488-labeled lysozyme to POPC LUVs prepared with a variable mol% of POPS was then examined quantitatively by FCS. In Fig. 2B, the fractional amplitude f_2 associated with POPC liposomes

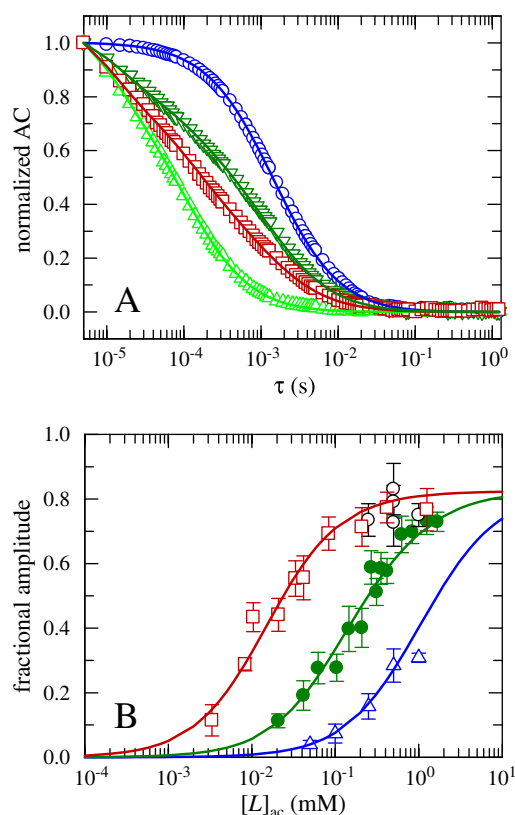


Fig. 2. FCS measurements of Alexa488-conjugated lysozyme binding to liposomes prepared with variable anionic phospholipid content. (A) Normalized AC curves of Alexa488-conjugated lysozyme (10 nM; $D/P=0.67$) in the absence (Δ) and in the presence of 0.42 (\square) and 1.25 mM (∇) POPC:POPS 80:20 LUVs and of BODIPY-PC-labeled liposomes prepared with the same lipidic composition (\circ). The lines through the data represent the best fit of Eqs. (4) and (6) to one- and two-component samples, respectively. (B) The experimental fractional amplitudes f_2 obtained for POPC liposomes containing 10 (Δ), 20 (\bullet), 30 (\square) and 50 (\circ) mol% of POPS are plotted as a function of the accessible lipid concentration. The solid curves are the best fit obtained in a global analysis of the binding data (10, 20 and 30 mol% POPS) according to a three-component model ($\mu=100,000$ and $q=1.9$ were fixed in the analysis): the fitting parameters were 0.4 nM for the concentration of free Alexa 488 dye and $K_p = (4.5 \pm 0.7) \times 10^4$, $K_p = (1.9 \pm 0.1) \times 10^5$ and $K_p = (7.0 \pm 0.4) \times 10^5$ for 10, 20 and 30 mol% POPS-containing liposomes, respectively (see the text for more details).

prepared with 10, 20 and 30 mol% of anionic POPS is plotted as a function of the accessible lipid concentration in the samples. Surprisingly, this parameter seems to reach a plateau value of $f_2^{\text{max}} \sim 0.80 < 1$, that persisted even when the acidic phospholipid content of the liposomes was increased to 50 mol% of POPS ($f_2 = 0.79 \pm 0.05$ for $[L]_{\text{ac}} = 2 \text{ mM}$). It should be noted that in this last case it was not possible to explore a wider range of phospholipid concentrations in the partitioning assay because of the Alexa488-lysozyme-induced liposome aggregation, which affects the form of the AC curves, as it is exemplified in Fig. S2. The plateau detected suggests that apparently as much as $\sim 20\%$ of a fluorescent species remains unbound in solution at saturating lipid concentrations. We considered three different explanations for this result, namely that (i) the labeling method inactivated lysozyme by inducing a conformational change of the protein, (ii) the chemical conjugation of the protein altered its binding behavior by changing its net charge, and finally (iii) the presence of vestigial free fluorophore in solution was responsible for this effect. To test for the first hypothesis, circular dichroism (CD) was used to characterize the secondary structure of lysozyme and ensure that the protein backbone was not drastically disturbed by covalently-binding of Alexa 488 to the protein. The far-UV CD spectra obtained for the unlabeled and labeled lysozymes were superimposable (Fig. S3), confirming that the labeled protein was always properly folded. We next considered the possibility that the alteration of

lysozyme net charge due to non-specific labeling of the protein surface-exposed amino groups by the succinimidyl ester of Alexa 488, might be changing its affinity toward the negatively charged liposomes. Theoretically, 7 amino groups on lysozyme, including the ϵ -amino group in lysine residues and the α -amino group at the N-terminus, might be reactive but several studies have already shown that the major modification sites are the more surface-exposed Lys-97 and Lys-33, followed by the amino group on the N-terminus and Lys-1 [32–34]. For low average labeling ratios it is reasonable to assume a Poisson distribution for the number of fluorophores per molecule, and therefore the probabilities of obtaining unmodified, singly, doubly and triply-labeled lysozyme molecules are $P(0)=0.51$, $P(1)=0.34$ (71% of the labeled species), $P(2)=0.11$ (24% of the labeled species) and $P(3)=0.03$ (5% of the labeled species), respectively, for a labeling efficiency of ~ 0.67 fluorophores/protein (Table 2). At pH = 7.4, the unmodified lysozyme has a net charge of 8.0 [35], which should decrease to +5, +2 and -1 upon the progressive conjugation of the enzyme with the fluorophore Alexa 488 [36]. Although the triply-labeled protein is present only in trace amounts in solution, its fractional contribution to the Alexa488-lysozyme AC curve might reach 0.22 (Table 2), close to the non-binding fraction detected in the partitioning experiments if it is further assumed that no self-quenching occurs between the covalently-bound fluorophores. To test for this correspondence, we explored different labeling conditions of lysozyme with Alexa 488. Both lowering the pH from 8.3 to 7.5 (to maximize the modification of the N-terminal group of the enzyme) or the use of an equimolar instead of 2:1 dye-to-protein ratio in the reaction mixture (to try to reduce the final yield of the multiply-labeled protein species formed) caused a decrease in the final D/P obtained (from 0.67 to 0.50 and 0.21, respectively (Table 2)). However, when the FCS measurements were repeated with these protein batches the apparent maximal fractional amplitude, f_2^{\max} , obtained did not register an increase equivalent to the expected change undergone by $f(3)$, the fractional amplitude associated with the triply-labeled lysozyme (which was expected to decrease from 0.22 to 0.04 when D/P changed from 0.67 to 0.21, Table 2). Therefore, we ruled out this possibility as the dominant factor and considered alternatively that the presence of some residual free Alexa dye in solution was responsible for this effect. This third explanation is considered in more detail in the next section.

4.3. Alexa 488 (free dye) binds non-covalently to lysozyme

Since the purification of the labeled protein by gel filtration chromatography under optimal chromatographic conditions seems to have failed to remove the unconjugated label completely, we considered that the anionic Alexa 488 dye could also be non-

covalently bound to the highly cationic lysozyme. This hypothesis was tested by monitoring the binding of the free Alexa 488 fluorophore to lysozyme by steady-state fluorescence measurements. Upon increasing the total lysozyme concentration in solution, the fluorescence intensity of 0.1 μM free unconjugated dye was found to progressively decrease (Fig. 3). Assuming the formation of a 1:1 complex between the enzyme and free dye, a $K_d = (99 \pm 6) \mu\text{M}$ and a quenching factor $F = 1.9$ were obtained by nonlinear fitting of Eq. (2) to the experimental data of I versus $[P]_t$ (Fig. 3). Concomitantly, the steady-state fluorescence anisotropy of the fluorophore underwent an approximately ten-fold increase, starting from $\langle r \rangle_t = 0.012$ for the free fluorophore, revealing the progressive association of the dye to its protein binding site (Fig. 3). The nonlinear fitting of Eq. (3) to the experimental data of $\langle r \rangle_t$ versus $[P]_t$ yielded an equilibrium dissociation constant $K_d = (94 \pm 6) \mu\text{M}$ and $\langle r \rangle_b = 0.140 \pm 0.003$. Lysozyme has already been reported to form a stoichiometric 1:1 complex with the fluorescent dye eosin Y, a tetrabrominated derivative of fluorescein [37,38]. Eosin binds in a hydrophobic pocket of lysozyme distinct from its active site [37], with a $K_d = 4.5 \mu\text{M}$ at pH 5.3 [38]. The much weaker affinity of Alexa 488 relatively to eosin toward lysozyme can be explained by its more hydrophilic character.

In conclusion, in addition to the covalently-tagged Alexa 488 fluorophore, lysozyme is also able to form a 1:1 non-covalent complex with this probe. Prior to an FCS measurement, the fluorescently-labeled lysozyme was diluted to a much lower concentration, around 10–40 nM, causing the dissociation of Alexa 488 fluorophore from the protein. The anionic fluorophore remains free in solution and does not bind to the negatively-charged liposomes due to the strong repulsive electrostatic interactions between these two components at pH 7.4 [39]. In fact, the re-analysis of the AC curves measured for each batch of Alexa488-lysozyme using a two- instead of one-component model (Eq. (6)) slightly improved the quality of the fits. After fixing the pre-determined diffusion time associated with the free dye in each analysis, an average diffusion time $\tau_2 = 108 \pm 3 \mu\text{s}$ was obtained for the Alexa488-conjugated protein. Considering $D_{\text{Rhodamine 110}} = 440 \mu\text{m}^2 \text{s}^{-1}$ [27], $D_{\text{Alexa488-lysozyme}} = 83 \pm 7 \mu\text{m}^2 \text{s}^{-1}$ was calculated, close to the experimental value of $D = 109 \mu\text{m}^2 \text{s}^{-1}$ measured for lysozyme [40]. More importantly, the recovered average fractional amplitudes f_i associated with the diffusion of free dye in solution presented a good agreement with the plateau reached in each set of partitioning experiments carried out with the different protein batches, corroborating the above conclusion (e.g. $f_1 = 0.21 \pm 0.08$ for Alexa488-conjugated lysozyme with a $D/P = 0.67$).

Further evidence in favor of the third hypothesis was obtained from an additional set of experiments. A second gel filtration chromatography using a high ionic strength buffer was carried out to further purify a

Table 2

Poisson statistics for the number of fluorophores covalently-bound per lysozyme molecule. Poisson probabilities of having lysozyme molecules labeled with 0, 1, 2 and 3 Alexa Fluor 488 fluorophores, $P(i)$, normalized probabilities for the fluorescently-labeled enzyme molecules only, $P_n(i)$, and fractional amplitudes of the AC curve associated with each fluorescently-labeled protein species, $f(i)$, as a function of the final average labeling molar ratio, D/P , of the sample.

Labeling conditions	Poisson probabilities	Normalized probabilities			Fractional amplitudes ^a							
		$P(0)$	$P(1)$	$P(2)$	$P_n(1)$	$P_n(2)$	$P_n(3)$	$f(1)$	$f(2)$	$f(3)$		
1:1 ^b	8.3	0.21	0.81	0.17	0.02	0.00	0.90	0.09	0.01	0.67	0.28	0.04
2:1	7.5	0.50	0.61	0.30	0.08	0.01	0.77	0.19	0.03	0.42	0.42	0.16
2:1	8.3	0.67	0.51	0.34	0.11	0.03	0.71	0.24	0.05	0.33	0.44	0.22

^a The fractional amplitudes were calculated considering that the protein brightness scales linearly with the number of fluorophores per molecule (i.e. no self-quenching occurs).

^b Dye-to-protein molar ratio used in the labeling reaction.

^c pH used in the labeling reaction.

^d Final dye-to-protein molar ratio of the sample determined spectrophotometrically.

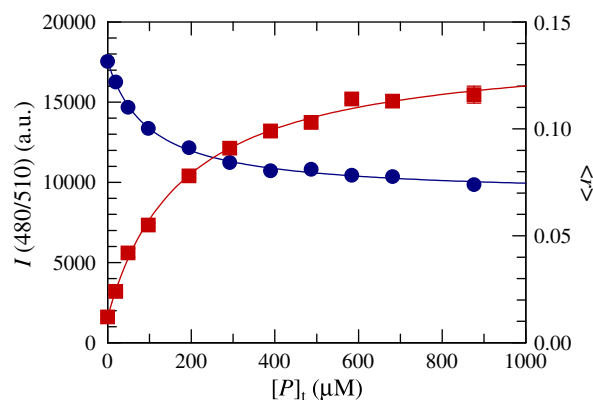


Fig. 3. Alexa 488 (free dye) binds non-covalently to lysozyme. Dependence of the steady-state fluorescence intensity, I (●) and anisotropy, $\langle r \rangle_t$ (■) of 0.1 μM Alexa 488 with lysozyme concentration in solution, $[P]_t$. The solid curves are the best fits of Eqs. (2) and (3) to the data of I and $\langle r \rangle_t$ versus $[P]_t$, respectively.

batch of Alexa488-lysozyme ($D/P=0.45$). The chromatogram and fluorescence spectra presented in Fig. S4 confirm that the addition of 0.3 M NaCl to the buffer solution was able to induce the dissociation of Alexa 488 dye (peak II) from the fluorescently-labeled protein (peak I). After pooling and extensively dialyzing peak I against 20 mM Hepes-KOH, 0.1 mM EDTA, pH 7.4 buffer, additional FCS measurements were performed. In the presence of 4 mM POPC:POPS 80:20 LUVs, $f_{ves}^{M2} = (75 \pm 10)\%$ was measured for the non-purified batch of conjugated protein, in agreement with $f_{ves}^{M2} = (73 \pm 3)\%$ obtained earlier for Alexa488-lysozyme ($D/P=0.67$) (Fig. 2B). When these measurements were repeated using now the purified conjugated protein pool (F11 + F12), a higher value of $f_{ves}^{M2} = (90 \pm 5)\%$ was obtained (data not shown). This result conclusively shows that the residual free Alexa 488 dye present in the Alexa 488 fluorescently-labeled lysozyme samples was responsible for an apparent maximal binding level lower than 100% obtained earlier in the FCS partitioning curves.

4.4. Analysis of FCS partitioning curves in the presence of a non-binding component

To evaluate how much the presence of a non-binding component affects the protein partition curves measured by FCS, partitioning curves were again simulated for 10 nM fluorescently-labeled protein ($K_p = 1 \times 10^6$) but now in the presence of 0.5 nM free dye (three-component model, M3). According to the master Eq. (7) for a multicomponent system, and using the same set of assumptions as before (see the Theory section), it can be derived that the absolute amplitudes of each diffusing particle are given by Eqs. (19.A), (19.B) and (19.C), respectively,

$$A_{Dye}^{M3} = \frac{q^2 \cdot N_{Dye}}{T} \quad (19.A)$$

$$A_p^{M3} = \frac{N_p^f}{T} \quad (19.B)$$

$$A_{ves}^{M3} = \frac{\left(\sum_{k=1}^l k^2 \cdot P(k, <k>) \right) \cdot N_{ves}^t}{T} \quad (19.C)$$

where $T = q \cdot N_{Dye} + N_p^f + \left(\sum_{k=1}^l k \cdot P(k, <k>) \right) \cdot N_{ves}^t$, N_{Dye} is the mean number of free dye molecules in solution and q is the ratio of the brightness of the free dye to that of the fluorescently-labeled protein. Furthermore, the fractional amplitude associated with the slowest diffusing species, f_{ves}^{M3} , of this three-component system can be calculated using Eq. (20):

$$f_{ves}^{M3} = \frac{\left(\sum_{k=1}^l k^2 \cdot P(k, <k>) \right) \cdot N_{ves}^t}{q^2 \cdot N_{Dye} + N_p^f + \left(\sum_{k=1}^l k^2 \cdot P(k, <k>) \right) \cdot N_{ves}^t} \quad (20)$$

Assuming that the free fluorophore is two-fold brighter than the fluorescently-labeled protein ($q = 2$), the calculated partition curve of f_{ves}^{M3} versus $[L]_{ac}$ was found to strongly deviate from the usual hyperbolic behavior, leveling off to a limiting value of ~ 0.85 , much lower than 1, as expected (Fig. 1D). Accordingly a simple mole-fraction partition model (Eq. (9)) gave a poor fit to the simulated data ($K_p = 6.4 \times 10^6$; $\chi^2 = 6.9 \times 10^{-3}$ (Table 1)). The use of an empirical modified equation that accounts for the partitioning curves not reaching an asymptotic level of one [12]:

$$x_m = \frac{K_p \cdot [L]_{ac}}{[W] + K_p \cdot [L]_{ac}} \cdot x_m^{\max} \quad (21)$$

greatly improved the quality of the fit ($K_p = 1.0 \times 10^7$; $x_m^{\max} = 0.86$; $\chi^2 = 6.6 \times 10^{-5}$ (Table 1)). In Eq. (21), x_m^{\max} is the maximum fraction of membrane-binding competent species present in each sample (determined at lipid saturation). However, the K_p recovered was an order of magnitude higher than the input value used in the simulation, demonstrating that in this case proper analysis of the partitioning data must take into consideration a more complex, three-component model (Fig. 1D). Therefore, the experimental binding data obtained for each protein batch (f_2 versus $[L]_{ac}$ for 10, 20 and 30 mol% POPS containing liposomes) was globally fitted using the nonlinear least-squares procedure described in detail in Section 2.5.3. This procedure takes into account the probabilistic distribution of the membrane-binding species among the liposomes in addition to the presence of a non-membrane-binding component in solution. It is important to mention that although the simultaneous presence in solution of three fluorescent species with different diffusion coefficients (free dye, free fluorescently-labeled protein and lipid vesicles with at least one conjugated protein bound, respectively) implies that the analysis of the experimental AC curves should have been done using a three-component model (model M3 – Eq. (6)), we found that reliable partitioning data was still obtained when the experimental AC curves were fitted using a simplifying two-component equation (see the Supporting Information).

By implementing the data analysis strategy described above, the partition coefficients of Alexa488-lysozyme were found to increase exponentially with the mol% of POPS included in the POPC liposomes (Fig. 4), showing that electrostatic interactions dominate this association when a low ionic strength buffer is used. This exponential relationship was essentially independent of the lysozyme labeling ratio used (Fig. 4), supporting the view that the main non-binding component was correctly identified as the free dye in solution and that the labeling heterogeneity of the protein does not markedly influence its overall partitioning behavior. The concentrations of free Alexa 488 dye found for each protein batch used in the FCS measurements were 0.3, 1.7 and 0.4 nM for a $D/P = 0.21$, 0.50 and 0.67, respectively (or 3.5%, 12% and 5.6% relatively to the concentration of fluorescently-labeled protein present in each protein batch, respectively).

5. Discussion

5.1. Using FCS to measure partition coefficients

Rusu and co-workers [11] were the first authors to carry out a systematic binding study of fluorescently labeled peptides to lipid vesicles using FCS. This study validated the use of this technique by confirming that the partition coefficients obtained from their FCS

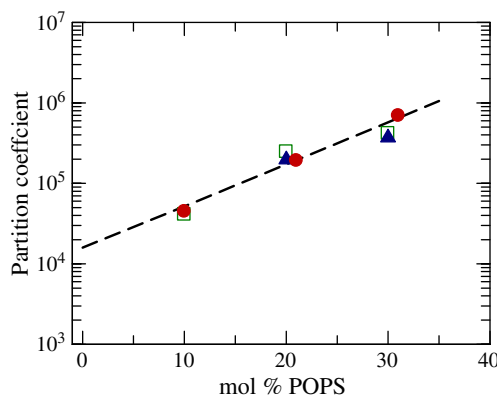


Fig. 4. Dependence of the Alexa488-lysozyme mole-fraction partition coefficients with the mol% of POPS included in the POPC LUVs. The straight line is the linear least-squares best fit to the data obtained using different protein batches: D/P of 0.21 (□), 0.50 (▲) and 0.67 (●).

measurements were comparable to those determined using more conventional techniques [11]. Since then, FCS has been increasingly applied to the study of interfacial partition to phospholipid vesicles of different peptide and proteins [12,39,41–51]. The pioneer work of Rusu et al. [11] established the conditions necessary for a correct quantitative analysis of the FCS binding data, namely fitting individual curves to a two-component AC function and extracting the fraction of bound peptide/protein by *only using the absolute amplitudes* of the free peptide and the total number of peptides in solution. Nevertheless, this recommendation has often been ignored in FCS partition studies. In this work, we show that when the function used in the fitting procedure employs fractional instead of absolute amplitudes as weighting factors (i.e., the fitting function most commonly available in the data analysis software programs), the correct analysis of the experimental binding data requires using a nonlinear iterative least-squares procedure that takes into account the statistical (Poissonian) distribution of the fluorescently-labeled protein among the ensemble of liposomes to not overestimate the recovered protein partition coefficients. The application of this method is expected to be particularly important for peptides or proteins that present high K_p values due to the establishment of strong Coloumbic interactions with anionic lipid membranes.

The FCS partition curves obtained in this study for the Alexa 488-conjugated lysozyme and extruded liposomes prepared with variable anionic lipid content always reached an asymptotic value lower than 100% (Fig. 2B). Some of the partitioning curves published in the literature also leveled off to a maximum value of the fraction of protein bound to the vesicles lower than 100% at lipid saturating conditions [12,45,47,48]. Ladokhin and co-workers elegantly showed in their work that this last result was due to a pH-dependent formation of a membrane-competent form of annexin B12 [12] and diphtheria toxin T-domain [45] – if the pH of the medium was sufficiently acidified, the fluorescently-labeled protein bound 100% to the phospholipid vesicles. On the other hand, Pu et al [47,48] justified their results by the preferential binding of the fluorescently-labeled phosphatidylinositol-specific phospholipase C to the smaller vesicles present in the polydisperse small unilamellar population used in their experiments. Regarding our own study, we showed that the non-binding component detected in the Alexa488-conjugated lysozyme partitioning curves is due to the presence of a trace amount of free Alexa 488 dye in solution that was not completely removed during the purification of the fluorescently-conjugated protein due to its non-covalent association with lysozyme. Upon dilution of the Alexa 488-conjugated protein to nM concentrations required to carry out the FCS measurements, the non-covalently-bound Alexa 488 dye is released from the protein and remains free in solution because both the fluorophore and the lipid vesicles are negatively-charged. The presence of vestigial free dye in solution is a common situation previously detected in several other FCS studies [52–55] due to the often encountered difficulty in completely removing it during the purification procedure necessary after labeling the species of interest with an adequate fluorophore for the FCS measurements. It should also be noted that the true molar fraction of the freely diffusing dye can be significantly under- or overestimated in the FCS measurements depending if its molecular brightness is significantly lower/higher than that of the fluorescently-conjugated protein itself, respectively ($q < 1$ or $q > 1$ in Eq. (19.A), respectively).

5.2. Lysozyme binding to anionic phospholipid vesicles

The partition coefficients determined by FCS for Alexa488-conjugated lysozyme presented an exponential dependence on the molar fraction of POPS included in the liposomes (Fig. 4), showing the predominance of electrostatic interactions in lysozyme binding to negatively charged liposomes and the relatively weak binding of the protein to electrically neutral bilayers, in general agreement with the literature [35,56]. In addition, the partition coefficients were found to be essentially independent of the final D/P obtained in the labeling reactions of lysozyme

($0.21 < D/P < 0.67$) indicating that the non-specific method used for fluorescently-labeling the protein did not alter dramatically its average binding behavior to the liposomes. However, our results are at variance with a recent publication from Gorbenko et al. [57] in two important aspects: (i) overall lysozyme binding to the liposomes was found to be much weaker in this study compared to Gorbenko's work, and (ii) the partitioning curves obtained here for Alexa 488-conjugated lysozyme did not present any deviation from the expected hyperbolic behavior when the liposomes included 20 and 30 mol% POPS in their composition (i.e. there was no evidence for Alexa488-conjugated lysozyme self-association upon membrane association within the lipid and protein concentrations used in our experiments). We speculate that the discrepancies between the two studies might be related to the simultaneous use of a much higher lysozyme concentration (150 nM) and much lower lipid total concentrations (that varied between 12 and 70 μ M) by Gorbenko et al. in their work [57]. These conditions are known to induce an extensive protein-mediated aggregation of the negatively-charged liposomes [23]. If this is the case, then the decrease detected in the fluorescence of the fluorescein 5'-isothiocyanate labeled lysozyme upon its binding to the liposomes by Gorbenko et al. in their study [57] might be reporting both processes simultaneously and not only the lipid binding properties of the protein. In this respect, it should be noted that the very high sensitivity of the FCS technique enables high signal-to-noise measurements at very low (nanomolar) concentrations of fluorescently-labeled peptides/proteins and therefore the binding of the protein/peptide to the liposomes does not usually change significantly the surface charge density of the vesicles, decreasing the probability of an extensive protein-mediated aggregation of the lipid vesicles. Furthermore, even when this phenomenon occurs, it can be easily detected in the FCS measurements because it produces an alteration in the shape of the experimental AC curves, as it is exemplified in Fig. S2. Therefore, FCS measurements can guarantee that protein partition is evaluated under conditions that completely eliminate the often concomitant phenomenon of protein-induced liposome aggregation, which might complicate data analysis.

6. Conclusions

In this work, we re-evaluate the conditions required for a correct quantitative analysis of FCS partition data. There were two major findings: (1) in order to avoid obtaining biased partition coefficients, the Poissonian loading of the lipid vesicles with the fluorescently-labeled peptide or protein must be taken explicitly into account when fitting a partition model to the experimental binding curves obtained by the FCS technique (fractional amplitude of the bound species *versus* accessible lipid concentration) and, (2) the presence of a trace amount of free fluorescent dye (non-binding component) in the system can lead to plateau values lower than 100% in the partition curves obtained using the FCS technique. A misinterpretation of this result can lead to a large overestimation of the recovered partition coefficients. Finally, FCS measurements of lysozyme binding to POPS-containing liposomes were easily uncoupled from the potential interference of lysozyme-mediated liposome aggregation, confirming that its binding is dominantly driven by electrostatic interactions.

Acknowledgments

We thank Nidia Estrela for her help in the CD measurements.

The authors acknowledge Fundação para a Ciência e Tecnologia (Project PTDC/QUI-BIQ/099947/2008 and Ph.D. grant SFRH/BD/61723/2009 to A.M.) for financial support.

Appendix A. Supplementary data

Supplementary data to this article can be found online at doi:10.1016/j.bbmem.2011.06.001.

References

- [1] W.H. Cho, R.V. Stahelin, Membrane-protein interactions in cell signaling and membrane trafficking, *Annu. Rev. Biophys. Biomolec. Struct.* 34 (2005) 119–151.
- [2] J.T. Groves, J. Kuriyan, Molecular mechanisms in signal transduction at the membrane, *Nat. Struct. Mol. Biol.* 17 (2010) 659–665.
- [3] S. McLaughlin, D. Murray, Plasma membrane phosphoinositide organization by protein electrostatics, *Nature* 438 (2005) 605–611.
- [4] A. Mulgrew-Nesbitt, K. Diraviyam, J.Y. Wang, S. Singh, P. Murray, Z.H. Li, L. Rogers, N. Mirkovic, D. Murray, The role of electrostatics in protein–membrane interactions, *Biochim. Biophys. Acta* 1761 (2006) 812–826.
- [5] G.P. Gorbenko, P.K.J. Kinnunen, The role of lipid–protein interactions in amyloid-type protein fibril formation, *Chem. Phys. Lipids* 141 (2006) 72–82.
- [6] C. Aisenbrey, T. Borowik, R. Byström, M. Bokvist, F. Lindström, H. Misiak, M.A. Sani, G. Gröbner, How is protein aggregation in amyloidogenic diseases modulated by biological membranes? *Eur. Biophys. J. Biophys. Lett.* 37 (2008) 247–255.
- [7] J.A. Hebda, A.D. Miranker, The interplay of catalysis and toxicity by amyloid intermediates on lipid bilayers: insights from type II diabetes, *Ann. Rev. Biophys.* 38 (2009) 125–152.
- [8] S.M. Butterfield, H.A. Lashuel, Amyloidogenic protein membrane interactions: mechanistic insight from model systems, *Angew. Chem. – Int. Edit.* 49 (2010) 5628–5654.
- [9] C. Aisenbrey, B. Bechinger, G. Gröbner, Macromolecular crowding at membrane interfaces: adsorption and alignment of membrane peptides, *J. Mol. Biol.* 375 (2008) 376–385.
- [10] N.C. Santos, M. Prieto, M.A.R.B. Castanho, Quantifying molecular partition into model systems of biomembranes: an emphasis on optical spectroscopic methods, *Biochim. Biophys. Acta* 1612 (2003) 123–135.
- [11] L. Rusu, A. Gambhir, S. McLaughlin, J. Rädler, Fluorescence correlation spectroscopy studies of peptide and protein binding to phospholipid vesicles, *Biophys. J.* 87 (2004) 1044–1053.
- [12] Y.O. Posokhov, M.V. Rodnin, L. Lu, A.S. Ladokhin, Membrane insertion pathway of annexin B12: thermodynamic and kinetic characterization by fluorescence correlation spectroscopy and fluorescence quenching, *Biochemistry* 47 (2008) 5078–5087.
- [13] O. Krichevsky, G. Bonnet, Fluorescence correlation spectroscopy: the technique and its applications, *Rep. Prog. Phys.* 65 (2002) 251–297.
- [14] J.R. Lakowicz, *Principles of Fluorescence Spectroscopy*, third ed. Springer, New York, 2006.
- [15] S.T. Hess, S.H. Huang, A.A. Heikal, W.W. Webb, Biological and chemical applications of fluorescence correlation spectroscopy: a review, *Biochemistry* 41 (2002) 697–705.
- [16] E. Haustein, P. Schwille, Fluorescence correlation spectroscopy: novel variations of an established technique, *Annu. Rev. Biophys. Biomolec. Struct.* 36 (2007) 151–169.
- [17] C.C.F. Blake, D.F. Koenig, G.A. Mair, A.C.T. North, D.C. Phillips, V.R. Sarma, Structure of hen egg-white lysozyme – a 3-dimensional Fourier synthesis at 2 Å resolution, *Nature* 206 (1965) 757–761.
- [18] H.R. Ibrahim, U. Thomas, A. Pellegrini, A helix-loop-helix peptide at the upper lip of the active site cleft of lysozyme confers potent antimicrobial activity with membrane permeabilization action, *J. Biol. Chem.* 276 (2001) 43767–43774.
- [19] H.X. Zhao, E.K.J. Tuominen, P.K.J. Kinnunen, Formation of amyloid fibers triggered by phosphatidylserine-containing membranes, *Biochemistry* 43 (2004) 10302–10307.
- [20] H.X. Zhao, A. Jutila, T. Nurminen, S.A. Wickstrom, J. Keski-Oja, P.K.J. Kinnunen, Binding of endostatin to phosphatidylserine-containing membranes and formation of amyloid-like fibers, *Biochemistry* 44 (2005) 2857–2863.
- [21] J.M. Alakoskela, A. Jutila, A.C. Simonsen, J. Pirneskoski, S. Pyhäjoki, R. Turunen, S. Marttila, O.G. Mouritsen, E. Goormaghtigh, P.K.J. Kinnunen, Characteristics of fibers formed by cytochrome c and induced by anionic phospholipids, *Biochemistry* 45 (2006) 13447–13453.
- [22] N.L. Thompson, Fluorescence correlation spectroscopy, in: J. Lakowicz (Ed.), *Topics in Fluorescence Spectroscopy, Techniques*, Vol 1, Plenum Press, New York, 1991, pp. 337–378.
- [23] A. Coutinho, L.M.S. Loura, A. Fedorov, M. Prieto, Pinched multilamellar structure of aggregates of lysozyme and phosphatidylserine-containing membranes revealed by FRET, *Biophys. J.* 95 (2008) 4726–4736.
- [24] R.P. Haugland, *The Handbook. A Guide to Fluorescent Probes and Labeling Technologies*, 10th ed, 2005 Eugene, OR.
- [25] C.N. Pace, F. Vajdos, L. Fee, G. Grimsley, T. Gray, How to measure and predict the molar absorption-coefficient of a protein, *Protein Sci.* 4 (1995) 2411–2423.
- [26] L.D. Mayer, M.J. Hope, P.R. Cullis, Vesicles of variable sizes produced by a rapid extrusion procedure, *Biochim. Biophys. Acta* 858 (1986) 161–168.
- [27] P.O. Gendron, F. Avaltroni, K.J. Wilkinson, Diffusion coefficients of several rhodamine derivatives as determined by pulsed field gradient-nuclear magnetic resonance and fluorescence correlation spectroscopy, *J. Fluoresc.* 18 (2008) 1093–1101.
- [28] J.M. Smaby, M.M. Momsen, H.L. Brockman, R.E. Brown, Phosphatidylcholine acyl unsaturation modulates the decrease in interfacial elasticity induced by cholesterol, *Biophys. J.* 73 (1997) 1492–1505.
- [29] S.H. White, W.C. Wimley, A.S. Ladokhin, K. Kristova, Protein folding in membranes: determining energetics of peptide-bilayer interactions, *Methods Enzymol.* 295 (1998) 62–87.
- [30] L.L. Yu, M.Y. Tan, B. Ho, J.L. Ding, T. Wohland, Determination of critical micelle concentrations and aggregation numbers by fluorescence correlation spectroscopy: aggregation of a lipopolysaccharide, *Anal. Chim. Acta* 556 (2006) 216–225.
- [31] E.L. Elson, Fluorescence correlation spectroscopy measures molecular transport in cells, *Traffic* 2 (2001) 789–796.
- [32] D. Suckau, M. Mak, M. Przybylski, Protein surface topology-probing by selective chemical modification and mass-spectrometric peptide-mapping, *Proc. Natl. Acad. Sci. U.S.A.* 89 (1992) 5630–5634.
- [33] V. Schnaible, M. Przybylski, Identification of fluorescein-5'-isothiocyanate-modification sites in proteins by electrospray-ionization mass spectrometry, *Bioconjug. Chem.* 10 (1999) 861–866.
- [34] C.A. Teske, R. Simon, A. Niebisch, J. Hubbuch, Changes in retention behavior of fluorescently labeled proteins during ion-exchange chromatography caused by different protein surface labeling positions, *Biotechnol. Bioeng.* 98 (2007) 193–200.
- [35] J.J. Bergers, M.H. Vingerhoeds, L. Vanbloois, J.N. Herron, L.H.M. Janssen, M.J.E. Fischer, D.J.A. Crommelin, The role of protein charge in protein lipid interactions – pH-dependent changes of the electrophoretic mobility of liposomes through adsorption of water-soluble, globular-proteins, *Biochemistry* 32 (1993) 4641–4649.
- [36] C.A. Teske, M. Schroeder, R. Simon, J. Hubbuch, Protein-labeling effects in confocal laser scanning microscopy, *J. Phys. Chem. B* 109 (2005) 13811–13817.
- [37] X.J. Jordanides, M.J. Lang, X.Y. Song, G.R. Fleming, Solvation dynamics in protein environments studied by photon echo spectroscopy, *J. Phys. Chem. B* 103 (1999) 7995–8005.
- [38] J.F. Baugher, L.I. Grosswei, C. Lewis, Intramolecular energy-transfer in lysozyme-eosin complex, *J. Chem. Soc., Faraday Trans. II* 70 (1974) 1389–1398.
- [39] E. Rhoades, T.F. Ramlall, W.W. Webb, D. Eliezer, Quantification of alpha-synuclein binding to lipid vesicles using fluorescence correlation spectroscopy, *Biophys. J.* 90 (2006) 4692–4700.
- [40] J.G. de la Torre, M.L. Huertas, B. Carrasco, Calculation of hydrodynamic properties of globular proteins from their atomic-level structure, *Biophys. J.* 78 (2000) 719–730.
- [41] L. Yu, J.L. Ding, B. Ho, T. Wohland, Investigation of a novel artificial antimicrobial peptide by fluorescence correlation spectroscopy: an amphipathic cationic pattern is sufficient for selective binding to bacterial type membranes and antimicrobial activity, *Biochim. Biophys. Acta* 1716 (2005) 29–39.
- [42] P. Sengupta, M.J. Ruano, F. Tebar, U. Golebiewska, I. Zaitseva, C. Enrich, S. McLaughlin, A. Villalobo, Membrane-permeable calmodulin inhibitors (e.g. W-7/W-13) bind to membranes, changing the electrostatic surface potential – dual effect of W-13 on epidermal growth factor receptor activation, *J. Biol. Chem.* 282 (2007) 8474–8486.
- [43] G. Blin, E. Margeat, K. Carvalho, C.A. Royer, C. Roy, C. Picart, Quantitative analysis of the binding of ezrin to large unilamellar vesicles containing phosphatidylinositol 4,5 bisphosphate, *Biophys. J.* 94 (2008) 1021–1033.
- [44] Y.O. Posokhov, M.V. Rodnin, S.K. Das, B. Pucci, A.S. Ladokhin, FCS study of the thermodynamics of membrane protein insertion into the lipid bilayer chaperoned by fluorinated surfactants, *Biophys. J.* 95 (2008) L54–L56.
- [45] A. Kyrychenko, Y.O. Posokhov, M.V. Rodnin, A.S. Ladokhin, Kinetic intermediate reveals staggered pH-dependent transitions along the membrane insertion pathway of the diphtheria toxin T-domain, *Biochemistry* 48 (2009) 7584–7594.
- [46] D. Williams, J. Vicogne, I. Zaitseva, S. McLaughlin, J.E. Pessin, Evidence that electrostatic interactions between vesicle-associated membrane protein 2 and acidic phospholipids may modulate the fusion of transport vesicles with the plasma membrane, *Mol. Biol. Cell* 20 (2009) 4910–4919.
- [47] M.M. Pu, X.M. Fang, A.G. Redfield, A. Gershenson, M.F. Roberts, Correlation of vesicle binding and phospholipid dynamics with phospholipase c activity. Insights into phosphatidylcholine activation and surface dilution inhibition, *J. Biol. Chem.* 284 (2009) 16099–16107.
- [48] M.M. Pu, M.F. Roberts, A. Gershenson, Fluorescence correlation spectroscopy of phosphatidylinositol-specific phospholipase c monitors the interplay of substrate and activator lipid binding, *Biochemistry* 48 (2009) 6835–6845.
- [49] Y.N. Antonenko, I.V. Perevoshchikova, L.L. Davydova, I.A. Agapov, V.G. Bogush, Interaction of recombinant analogs of spider silk proteins 1F9 and 2E12 with phospholipid membranes, *Biochim. Biophys. Acta* 1798 (2010) 1172–1178.
- [50] S. Elbaum-Garfinkle, T. Ramlall, E. Rhoades, The role of the lipid bilayer in tau aggregation, *Biophys. J.* 98 (2010) 2722–2730.
- [51] E.R. Middleton, E. Rhoades, Effects of curvature and composition on alpha-synuclein binding to lipid vesicles, *Biophys. J.* 99 (2010) 2279–2288.
- [52] E. Matayoshi, K. Swift, Applications of FCS to protein-ligand interactions: comparison with fluorescence polarization, in: R. Riegler, E.S. Elson (Eds.), *Fluorescence Correlation Spectroscopy. Theory and Applications*, Springer-Verlag, Berlin, 2001, pp. 84–98.
- [53] H. Xu, J. Frank, U. Trier, S. Hammer, W. Schroder, J. Behlke, M. Schäfer-Korting, J.F. Holzwarth, W. Saenger, Interaction of fluorescence labeled single-stranded DNA with hexameric DNA-helicase RepA: a photon and fluorescence correlation spectroscopy study, *Biochemistry* 40 (2001) 7211–7218.
- [54] T. Krouglova, J. Vercammen, Y. Engelborghs, Correct diffusion coefficients of proteins in fluorescence correlation spectroscopy. Application to tubulin oligomers induced by Mg²⁺ and paclitaxel, *Biophys. J.* 87 (2004) 2635–2646.
- [55] S. Nath, J. Meuvius, J. Hendrix, S.A. Carl, Y. Engelborghs, Early aggregation steps in alpha-synuclein as measured by FCS and FRET: evidence for a contagious conformational change, *Biophys. J.* 98 (2010) 1302–1311.
- [56] E.H.W. Pap, M.C. Houbiers, J.S. Santema, A. van Hoek, A.J.W.G. Visser, Quantitative fluorescence analysis of the adsorption of lysozyme to phospholipid vesicles, *Eur. Biophys. J. Biophys. Lett.* 24 (1996) 223–231.
- [57] G.P. Gorbenko, V.M. Ioffe, P.K.J. Kinnunen, Binding of lysozyme to phospholipid bilayers: evidence for protein aggregation upon membrane association, *Biophys. J.* 93 (2007) 140–153.